CACNA1H^{M1549V} Mutant Calcium Channel Causes Autonomous Aldosterone Production in HAC15 Cells and Is Inhibited by Mibefradil

Esther N. Reimer, Gudrun Walenda, Eric Seidel, and Ute I. Scholl

Department of Nephrology, Medical School, Heinrich Heine University Düsseldorf, 40225 Düsseldorf, Germany

We recently demonstrated that a recurrent gain-of-function mutation in a T-type calcium channel, CACNA1H^{M1549V}, causes a novel Mendelian disorder featuring early-onset primary aldosteronism and hypertension. This variant was found independently in five families. CACNA1H^{M1549V} leads to impaired channel inactivation and activation at more hyperpolarized potentials, inferred to cause increased calcium entry. We here aimed to study the effect of this variant on aldosterone production. We heterologously expressed empty vector, *CACNA1H^{WT}* and *CACNA1H^{M1549V}* in the aldosterone-producing adrenocortical cancer cell line H295R and its subclone HAC15. Transfection rates, expression levels, and subcellular distribution of the channel were similar between CACNA1H^{WT} and CACNA1H^{M1549V}. We measured aldosterone production by an ELISA and *CYP11B2* (aldosterone synthase) expression by real-time PCR. In unstimulated cells, transfection of *CACNA1H^{WT}* led to a 2-fold increase in aldosterone levels compared with vector-transfected cells. Expression of *CACNA1H^{M1549V}* caused a 7-fold increase in aldosterone levels. Treatment with angiotensin II or increased extracellular potassium levels further stimulated aldosterone production in both *CACNA1H^{WT}*- and *CACNA1H^{M1549V}*-transfected cells. Similar results were obtained for *CYP11B2* expression. Inhibition of CACNA1H channels with the T-type calcium channel blocker Mibefradil completely abrogated the effects of CACNA1H^{WT} and CACNA1H^{M1549V} on *CYP11B2* expression. These results directly link CACNA1H^{M1549V} to increased aldosterone production. They suggest that calcium channel blockers may be beneficial in the treatment of a subset of patients with primary aldosteronism. Such blockers could target CACNA1H or both CACNA1H and the L-type calcium channel CACNA1D that is also expressed in the adrenal gland and mutated in patients with primary aldosteronism. **(*Endocrinology* 157: 3016–3022, 2016)**

Primary aldosteronism (PA) (1) is the most common cause of secondary hypertension, with a prevalence of up to 11% in hypertension referral centers (2). PA is due to autonomous production of the steroid hormone aldosterone, which is physiologically produced in the zona glomerulosa, mainly in response to volume depletion (via angiotensin II) or hyperkalemia. Aldosterone increases renal and intestinal salt (re)absorption and potassium secretion. Excess production leads to hypertension and optional hypokalemia. The main causes of PA are bilateral adrenal hyperplasia, also known as idiopathic hyperaldosteronism, and aldosterone-producing adenomas. Familial hyperaldosteronism (FH) is rare, and all solved forms are inherited in an autosomal-dominant fashion (3). These include the following: 1) glucocorticoid-remediable aldosteronism (FH-I) (4), with crossing-over events between *CYP11B2* (aldosterone synthase) and *CYP11B1* (11β-hydroxylase) (4); 2) FH-III, with mutations in the inward rectifier potassium channel *KCNJ5* (5–7); and 3) a syndrome of PA, seizures, and neurological abnormalities caused by mutations in the voltage-gated L-type calcium channel *CACNA1D* (8).

ISSN Print 0013-7227 ISSN Online 1945-7170
Printed in USA

Received March 14, 2016. Accepted May 31, 2016.
First Published Online June 3, 2016

Abbreviations: CT, cycle threshold; EIA, enzyme immunoassay; FH, familial hyperaldosteronism; GFP, green fluorescent protein; IRES, internal ribosome entry site; PA, primary aldosteronism.

Recently, by sequencing the exomes of 40 children with PA diagnosed at age 10 years or younger, we discovered the identical, novel heterozygous germline mutation (M1549V) in the *CACNA1H* gene in five families (9). *CACNA1H* is expressed in the adrenal gland and encodes a T-type calcium channel that is activated by small depolarizing potentials. Electrophysiological studies in human embryonic kidney-293 cells demonstrated that the mutation leads to reduced channel inactivation and a shift of activation to less depolarized potentials. These effects were inferred to cause increased calcium influx in adrenal glomerulosa cells.

We here express $CACNA1H^{WT}$ and ^{M1549V} in the human adrenocortical cancer cell line H295R and its subclone HAC15 and demonstrate that $CACNA1H^{M1549V}$ increases aldosterone production and expression of the aldosterone synthase gene *CYP11B2*. We further show that these effects are abolished by treatment with the T-type calcium channel blocker Mibefradil, suggesting that similar compounds may be useful in the treatment of patients with $CACNA1H^{M1549V}$.

Materials and Methods

Cell culture and reagents

HAC15 cells were cultured at 37°C and 5% CO_2 in DMEM: F12 (1:1; Gibco, Life Technologies) supplemented with 5% Cosmic calf serum (Hyclone Laboratories), 1% penicillin/streptomycin, 1% insulin-transferrin-selenium, 1% nonessential amino acids, and 0.1% lipid mixture (all Gibco). NCI-H295R cells were cultured in DMEM/Ham's F12 medium (Gibco) supplemented with 2.5% Ultroser G (Pall Biosepra), 1% ITS+ premix (Corning) and 1% penicillin/streptomycin.

Angiotensin II and Mibefradil (Sigma-Aldrich) were dissolved in PBS and cell culture grade KCl (Sigma-Aldrich) in H_2O.

Plasmids

$CACNA1H^{WT}$ and $CACNA1H^{M1549V}$ cDNAs were subcloned from pCMV6-Entry (Origene) (9) into pCMV6-AC-IRES-*GFP*-Puro (Origene) using MluI and RsrII (New England Biolabs Inc). The plasmids were purified using the EndoFree Plasmid Maxi Kit (QIAGEN).

Transfection, treatment, and harvesting for ELISA and quantitative PCR

Two million HAC15 cells were transfected with 1 μg DNA using the Amaxa Cell Line Nucleofector Kit R and the Nucleofector I (program X-05) (Lonza) according to the manufacturer's instructions. Transfection was confirmed by fluorescence microscopy. Twenty-four hours after the transfection, Cosmic calf serum concentration was reduced to 0.1%. Forty-eight hours after the transfection, the medium was changed to serum-deprived medium containing 10 nM angiotensin II, 10 μM Mibefradil, 14 mM K^+ (total, by addition of KCl), or a vehicle control [PBS; Biochrom]). Seventy-two hours after the transfection, the cells and/or supernatants were harvested for aldosterone enzyme immunoassay (EIA) and isolation of protein or RNA.

Immunofluorescent analysis and flow cytometry of transiently transfected cells

Three million H295R cells were transfected with 3 μg plasmid DNA using the Nucleofector I Lonza, (kit R, program P-20), followed by 30 minutes of recovery in RPMI 1640 medium. For immunofluorescence, 5×10^5 cells were seeded onto Nunc Lab-Tek chamber slides (Thermo Fisher Scientific) in 1.5 mL H295R culture medium. Three days after the transfection, cells were fixed with 4% paraformaldehyde in PBS with 4% sucrose and stained with primary antibodies, rabbit α-$Ca_V3.2$ (number ACC-025; Alomone, 1:500) or mouse anti-FLAG M2 (number F3165, 1:200; Sigma-Aldrich). Secondary antibodies were goat antirabbit IgG (H + L) Alexa Fluor 647 conjugate, and goat antimouse IgG (H + L) Alexa Fluor 633 conjugate (number A-21052 and number A-21245, 1:250; both Thermo Fisher). Images were acquired with an LSM 510 Meta (Zeiss) and processed using the manufacturer's software.

For flow cytometry, cells were isolated by trypsination 48 hours after transfection. All stainings were performed in regular medium. The live cell population was identified after propidium iodide staining (5 ng/μL; Sigma-Aldrich), using the PerCP-Cy5.5 channel of a FACSCanto II flow cytometer (BD Biosciences). For FLAG analysis, cells were fixed (4% paraformaldehyde, 10 min), permeabilized (0.1% Saponin [Sigma-Aldrich], 5% fetal calf serum/PBS, 5 min), and stained with mouse anti-FLAG M2 (number F3165; Sigma-Aldrich; 1:200, 60 min on ice), followed by Alexa Fluor 633 conjugate (number A-21245; Thermo Fisher Scientific; 1:100, 60 min on ice). Alexa Fluor 633 was measured using the allophycocyanin channel and green fluorescent protein (GFP) using the fluorescein isothiocyanate channel. GFP fluorescence of unfixed transfected cells was recorded as the control. Results were analyzed using the FlowJo software.

RNA isolation and real-time PCR

Total RNA was harvested using the RNeasy Mini Kit (QIAGEN) according to the manufacturer's instructions. Two hundred nanograms of RNA were transcribed using the Quantitect reverse transcription kit (QIAGEN). Expression levels of *CYP11B2* and *GAPDH* were quantified in a 7300 real-time PCR system (Applied Biosystems) using the Taqman gene expression master mix (Applied Biosystems), published primers and probes for *CYP11B2* (10) and a commercial assay for *GAPDH* (number HS02758991_g1; Applied Biosystems). Samples were analyzed in triplicates. ΔΔCycle threshold (CT) values were calculated by normalization of ΔCT values, with average ΔCT values of PBS-treated empty vector-transfected cells as a reference.

Aldosterone EIA and protein

Aldosterone concentrations were determined using the aldosterone EIA kit (number 10004377; Cayman) according to the manufacturer's instructions. Two dilutions were measured in duplicates each. For values outside the assay range, both duplicates were removed from the analysis. Total protein levels were determined in duplicates from cell lysates using the Micro BCA protein assay kit (Thermo Scientific).

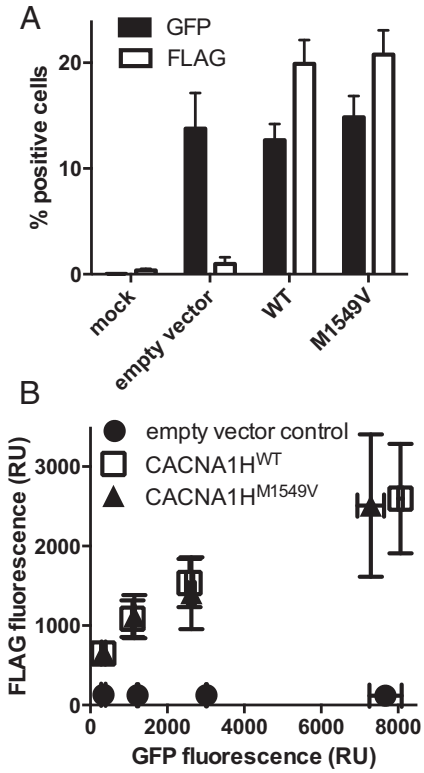

Figure 1. Flow cytometry of *CACNA1H*-transfected H295R cells. Cells were electroporated without DNA (mock), transfected with pCMV6-AC-IRES-*GFP*-Puro containing no insert (empty vector), FLAG-tagged *CACNA1H*^{WT} (WT), or FLAG-tagged *CACNA1H*^{M1549V} (M1549V). Cells were stained with a primary antibody against the FLAG epitope and a secondary antibody labeled with Alexa Fluor 633. A, The percentage of live cells positive for GFP or FLAG is similar for CACNA1H^{WT} and CACNA1H^{M1549V}. B, Among GFP-positive cells, FLAG median intensity was determined within bins of increasing GFP fluorescence (1–800, 800–2000, 2000–5000, and 5000–20 000 relative units [RUs]) and plotted against median GFP fluorescence. There was no significant difference in expression between *CACNA1H*^{WT} and *CACNA1H*^{M1549V} (see text) (n = 2 in bin 4 for *CACNA1H*^{WT} and *CACNA1H*^{M1549V}; n = 3 for all other data points). Error bars represent SEM.

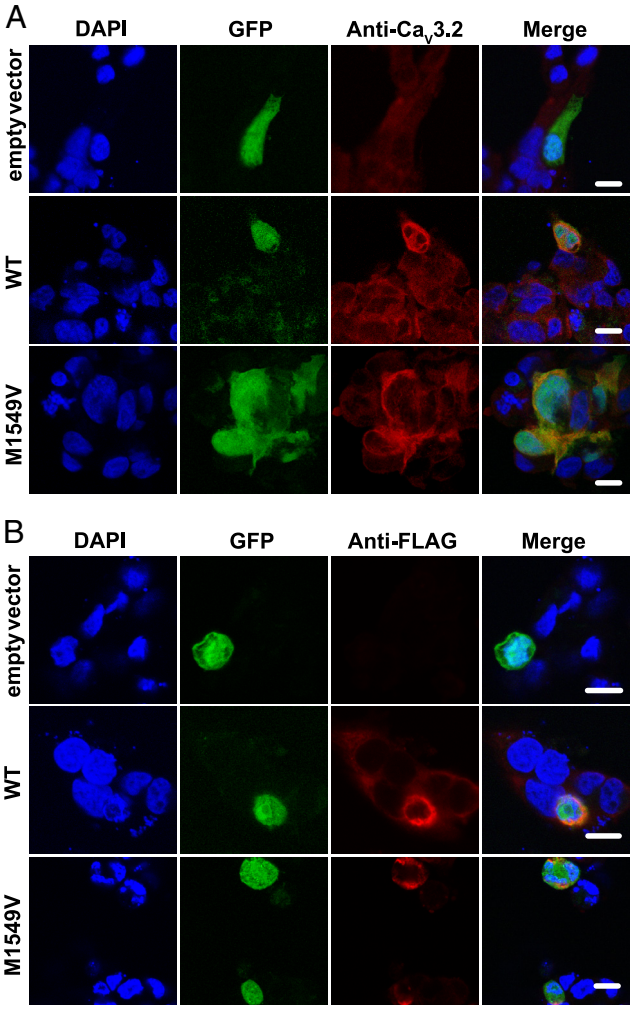

Figure 2. Immunofluorescent staining of *CACNA1H*-transfected H295R cells. Cells were transfected with pCMV6-AC-IRES-*GFP*-Puro containing no insert (empty vector), FLAG-tagged *CACNA1H*^{WT} (WT), or FLAG-tagged *CACNA1H*^{M1549V} (M1549V). DAPI nuclear staining is shown in blue, GFP fluorescence, denoting transfected cells, in green, and antibody staining in red. A, Cells were stained with an anti-Ca$_V$3.2 (CACNA1H) antibody (Alomone), demonstrating endogenous expression in all cells and stronger heterologous expression in *CACNA1H*-transfected cells (red). B, Cells were stained with an anti-FLAG antibody, demonstrating heterologous expression in *CACNA1H*-transfected cells only. *CACNA1H* transfection leads to overexpression of the tagged protein. Scale bars represent 10 μm. DAPI, 4′,6-diamino-2-phenylindole; WT, wild type.

Statistical analysis

Data were analyzed using the Prism software (GraphPad). *P* values were determined via an unpaired, two-tailed Student's *t* test in Prism (ELISA, quantitative PCR) or via a one-way ANOVA in the Microsoft Excel analysis tool (flow cytometry).

Results

The human NCI-H295R cell line, derived from a female patient with adrenocortical carcinoma (11, 12), is a commonly used model of aldosterone production. We used electroporation to transfect H295R cells with FLAG-tagged *CACNA1H*^{WT} and *CACNA1H*^{M1549V} in a vector containing the internal ribosome entry site (IRES) sequence and *GFP* (Figures 1 and 2). Transfection rates were assessed by flow cytometry (Figure 1A). The number of GFP-positive cells was greater than 12%, and no significant differences were observed between empty vector, *CACNA1H*^{WT}, and *CACNA1H*^{M1549V}. Similarly, we assessed the number of FLAG-positive cells, which was about 20% in both *CACNA1H*^{WT}- and *CACNA1H*^{M1549V}-transfected cells, with very little unspecific staining in the empty vector control. We then assessed median FLAG (approximated by AF633 fluorescence) and GFP expression within four bins of GFP expression after staining. There was no significant difference between CACNA1H^{WT} and CACNA1H^{M1549V} regarding GFP or AF633 fluorescence, suggesting that expression levels are similar (Figure 1B and

Supplemental Table 1). Next, we assessed the subcellular distribution of CACNA1H^{WT} and CACNA1HM1594V. By immunofluorescence with a native CACNA1H antibody, endogenous expression was detected in empty vector-transfected cells, consistent with previous studies using both electrophysiology and real-time PCR (13, 14). Confocal microscopy localized most of the channels to intracellular compartments (Figure 2A). Transfection of *CACNA1H* substantially increased expression levels without changing the expression pattern, with similar results for CACNA1H^{WT} and CACNA1H^{M1549V}. Immunofluorescence with an anti-FLAG antibody specifically stained heterologously transfected cells (Figure 2B).

To assess effects of CACNA1H^{WT} and CACNA1H^{M1549V} on aldosterone production, we transfected HAC15 cells, a subclone of NCI-H295R that has previously been used to assess the effect of mutant channels on aldosterone production (15–18). Cells were serum starved, and aldosterone levels were measured in the supernatant by an ELISA (Figure 3A). Compared with empty vector-transfected cells, CACNA1H^{WT}-expressing cells showed a 1.96-fold increase in aldosterone levels (23.93 ± 1.08 pg/μg protein vs 12.23 ± 0.53 pg/μg protein, $P < .0001$, n = 4 independent transfections for all ELISA results). Importantly, the expression of CACNA1H^{M1549V} increased aldosterone production even further (3.70-fold of CACNA1H^{WT}, 88.58 ± 5.57 pg/μg protein, $P < .0001$), consistent with a gain of function (Figure 3A). Because no angiotensin II was administered to the serum-starved cells, the conditions resemble the in vivo situation in PA, with suppressed renin and angiotensin levels. The results demonstrate that CACNA1H^{M1549V} can cause autonomous aldosterone production in the absence of depolarizing stimuli.

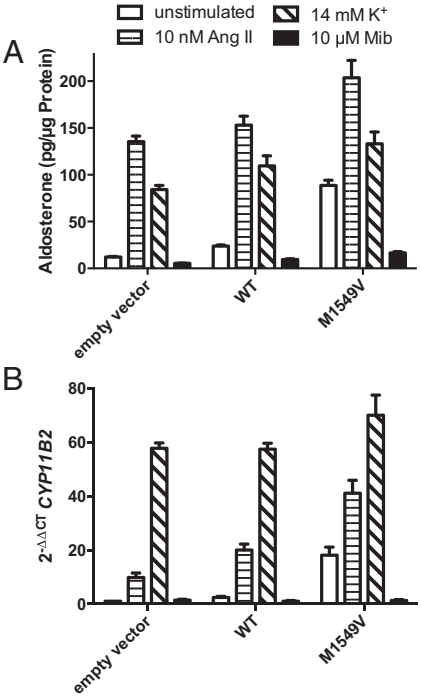

Figure 3. CACNA1H^{M1549V} causes increased aldosterone production in HAC15 cells that is abolished by Mibefradil. A, HAC15 cells were transfected with pCMV6-AC-IRES-*GFP*-Puro containing no insert (empty vector), *CACNA1H^{WT}* (WT), or *CACNA1H^{M1549V}* (M1549V). Cells were starved for 24 hours, followed by treatment with the indicated compounds for 24 hours. Aldosterone was measured from supernatants by an ELISA and normalized to protein levels. B, *CYP11B2* expression was measured by real-time PCR, with *GAPDH* as a reference gene. Unstimulated, treatment with PBS; Ang II, treatment with angiotensin II; K^+, treatment with KCl; Mib, treatment with the T-type calcium channel inhibitor Mibefradil (n = 4 for all groups). Error bars represent SEM. WT, wild type.

To examine the effects of such depolarizing stimuli on CACNA1H^{WT}- and CACNA1H^{M1549V}-expressing cells, we incubated cells with 10 nM angiotensin II, a concentration previously shown to increase aldosterone production (19). Angiotensin II led to significant increases in aldosterone production in all groups ($P < .0001$ for all). Angiotensin II-stimulated *CACNA1H^{M1549V}*-transfected cells produced significantly more aldosterone than angiotensin II-stimulated *CACNA1H^{WT}*-transfected cells (203.71 ± 18.47 pg/μg protein vs 153.07 ± 9.63 pg/μg protein, $P = .018$), but the relative increase in response to angiotensin II was smaller for CACNA1H^{M1549V} than for CACNA1H^{WT} (2.30-fold vs 6.40-fold).

Next, we examined the effect of increased extracellular potassium levels. After stimulation with 14 mM K^+ (19), aldosterone production increased in cells transfected with empty vector, *CACNA1H^{WT}* (both $P < .0001$) and *CACNA1H^{M1549V}* ($P = .0015$), with a smaller relative increase for *CACNA1H^{M1549V}* (1.50-fold vs 4.58-fold for CACNA1H^{WT}).

Lastly, we investigated whether the gain-of-function effects of the CACNA1H^{M1549V} variant can be blocked by pharmacological intervention. Treatment with Mibefradil, a potent CACNA1H blocker (20), significantly decreased aldosterone production in empty vector-transfected cells (5.43 ± 0.17 pg/μg protein vs 12.23 ± 0.53 pg/μg protein in untreated cells, $P < .0001$), in line with published data from cultured bovine glomerulosa cells (21). More importantly, Mibefradil significantly reduced the increased aldosterone production caused by transfection of *CACNA1H^{WT}* (9.51 ± 0.73 pg/μg protein vs 23.93 ± 1.08 pg/μg protein in untreated cells, $P < .0001$) and *CACNA1H^{M1549V}* (16.63 ± 1.32 pg/μg protein vs 88.58 ± 5.57 pg/μg protein, $P < .0001$).

Next, we assessed the expression levels of *CYP11B2* (aldosterone synthase), the rate-limiting enzyme in aldosterone biosynthesis, by real-time PCR (Figure 3B).

Transfection of *CACNA1H^{WT}* increased *CYP11B2* levels by a factor of 2.49 compared with cells transfected with empty vector. Transfection of *CACNA1H^{M1549V}*

Table 1. Antibody Table

Peptide/ Protein Target	Antigen Sequence (if Known)	Name of Antibody	Manufacturer, Catalog Number, and/or Name of Individual Providing the Antibody	Species Raised (Monoclonal or Polyclonal)	Dilution Used
$Ca_V3.2$	CHVEGPQERARVAHS	Anti-$Ca_V3.2$	Alomone, #ACC-025	Rabbit, polyclonal	1:500
FLAG	DYKDDDDK	Anti-FLAG M2	Sigma-Aldrich, #F3165	Mouse, monoclonal	1:200
Mouse IgG		Goat anti-Mouse IgG (H+L) Secondary Antibody, Alexa Fluor® 633 conjugate	ThermoFisher, #A-21052	Goat, polyclonal	1:250
Rabbit IgG		Goat anti-Rabbit IgG (H+L) Secondary Antibody, Alexa Fluor® 647 conjugate	ThermoFisher, #A-21245	Goat, polyclonal	1:250

further increased levels by a factor of 7.10 compared with CACNA1H^{WT} ($P = .0072$), again compatible with a gain-of-function effect of the mutant channel. Similar to the results of aldosterone ELISAs, treatment with angiotensin II further stimulated *CYP11B2* expression, with a larger relative effect on CACNA1H^{WT} (9.12-fold, $P = .0048$) than on CACNA1H^{M1549V} (2.30-fold, $P = .0107$). The stimulatory effect of treatment with KCl on *CYP11B2* expression was larger than the effect on aldosterone in the supernatant. Treatment of *CACNA1H^{WT}*- or *CACNA1H^{M1549V}*-transfected cells with Mibefradil suppressed *CYP11B2* expression to the same levels observed in empty vector-transfected cells.

Discussion

We here show that CACNA1H^{M1549V} causes autonomous aldosterone production by stimulation of *CYP11B2* expression.

In line with previous reports (22, 23), CACNA1H channels were found in intracellular compartments. Modulation of channel trafficking may play a role in the regulation of calcium entry.

Remarkably, the gain-of-function effect of CACNA1H^{M1549V} is more pronounced in the absence of stimulatory factors (angiotensin II and increased extracellular potassium concentration) than in their presence, suggesting that CACNA1H^{M1549V} activates the same pathways that are up-regulated by physiological stimulation of aldosterone production. This is interesting with regard to salt intake. Whereas aldosterone production physiologically decreases on a high-salt diet, our in vitro data suggest that aldosterone levels will remain elevated in subjects with the *CACNA1H^{M1549V}* variant, leading to volume expansion and hypertension. Conversely, a low-salt diet may prevent the manifestation of hypertension and explain incomplete penetrance of the condition (9).

The magnitude of the effect on aldosterone production observed in HAC15 cells could be an underestimate compared with the in vivo situation because *CACNA1H^{M1549V}* appears to cause microscopic adrenal hyperplasia, increasing not only the aldosterone production per cell but also the number of aldosterone-producing cells (9). Low transient transfection efficiencies are common for large cDNAs (~7 kb for *CACNA1H*) and may lead to an underestimation of aldosterone production. The rate of FLAG-positive cells could be higher than that of GFP-positive cells due to lower expression of GFP downstream of IRES (24). Preferential damage of transfected cells during staining may also play a role because the number of GFP-positive cells was higher in unfixed cells (Supplemental Figure 1).

The effects on aldosterone production are mediated by the increased expression of aldosterone synthase, likely via increased calcium signaling. Hyperplasia is probably similarly mediated by chronically increased calcium signaling (25). We observed slight differences in the magnitude of the effects between aldosterone levels in the supernatant (Figure 3A) and *CYP11B2* expression levels (Figure 3B). This is likely due to the shorter half-life of *CYP11B2* mRNA (~3 h in H295R cells [26]) compared with aldosterone in the supernatant. A delay in the reduction of aldosterone production explains why treatment with Mibefradil abrogates the effect of *CACNA1H^{WT}* and *CACNA1H^{M1549V}* transfection on *CYP11B2* expression but not on aldosterone levels. Similar explanations apply to the differential stimulatory effect of angiotensin II and KCl on *CYP11B2* expression levels vs aldosterone levels. *CYP11B2* expression has been shown to peak about 12 hours after the addition of angiotensin II and decrease thereafter. In contrast, potassium stimulation causes increasing *CYP11B2* levels, even after 40 hours (27). At 24 hours, *CYP11B2* expression and promoter activity were shown to be lower after angiotensin II stimulation than after potassium stimulation, yet total aldosterone in the

supernatant was higher after angiotensin II stimulation than after potassium stimulation (27, 28), in line with our data.

It is interesting to note that the transfection of *CACNA1H*^{WT} leads to an increase in aldosterone production, even in the absence of depolarizing stimuli such as angiotensin II or elevated extracellular potassium concentrations and that Mibefradil decreases the aldosterone production of empty vector-transfected cells. Our results suggest that the HAC15 membrane potential is at least temporarily depolarized enough to allow for the activation of endogeneous and heterologously expressed CACNA1H (threshold −60 mV) (29). In native glomerulosa cells, such potentials are reached during spontaneous membrane oscillations (30). Prior studies have demonstrated that Mibefradil and the dual L-type/T-type calcium channel blocker efonidipine can abrogate angiotensin II and potassium-induced aldosterone production, demonstrating that calcium influx through T-type channels is essential for the response to these stimuli (31).

Even though Mibefradil was withdrawn from the market due to drug interactions (32), the sustained response to Mibefradil in our experiments suggests that T-type calcium channel inhibitors may be a useful treatment option for patients with *CACNA1H* gain-of-function mutations. Treatment of hypertensive patients with 100 and 200 mg Mibefradil daily leads to mean plasma concentrations of approximately 2 μM and approximately 3 μM, respectively (33). The 10-μM concentration in our study will achieve virtually complete channel inhibition, whereas 3 μM concentrations result in approximately 80% channel inhibition (20). Whether T-type calcium channel inhibitors would be useful for the treatment of PA in the general population, however, is doubtful, given the lack of effect on aldosterone levels (34, 35), which could be due to overlapping function of CACNA1D (8, 36). Combined L- and T-type channel blockers may be more promising (37, 38), but further studies are warranted.

Acknowledgments

We thank Drs Rainer Haas, Ron-Patrick Cadeddu, and Stefanie Geyh (Heinrich Heine University Düsseldorf) for providing the Amaxa nucleofector; Dr Häussinger (Düsseldorf) for providing the FACSCanto II flow cytometer; Dr William Rainey (University of Michigan) for his kind gift of the HAC15 cell line; and Dr Matthias Haase (Düsseldorf) for the H295R cell line. Microscopy was performed at the Düsseldorf Center for Advanced imaging.

Address all correspondence and requests for reprints to: Ute I. Scholl, MD, Department of Nephrology, Medical School, Heinrich Heine University, Moorenstraße 5, 40225 Düsseldorf, Germany. E-mail: ute.scholl@med.uni-duesseldorf.de.

This work was supported by NRW-Rückkehrerprogramm and Junges Kolleg der Nordrhein-Westfälischen Akademie der Wissenschaften und der Künste (both Ministerium für Innovation, Wissenschaft und Forschung des Landes Nordrhein-Westfalen, Germany, to U.I.S.).

Disclosure Summary: The authors have nothing to disclose.

References

1. **Conn JW.** Presidential address. I. Painting background. II. Primary aldosteronism, a new clinical syndrome. *J Lab Clin Med*. 1955;45:3–17.
2. **Rossi GP, Bernini G, Caliumi C, et al.** A prospective study of the prevalence of primary aldosteronism in 1,125 hypertensive patients. *J Am Coll Cardiol*. 2006;48:2293–2300.
3. **Korah HE, Scholl UI.** An update on familial hyperaldosteronism. *Horm Metab Res*. 2015;47:941–946.
4. **Lifton RP, Dluhy RG, Powers M, et al.** A chimaeric 11 β-hydroxylase/aldosterone synthase gene causes glucocorticoid-remediable aldosteronism and human hypertension. *Nature*. 1992;355:262–265.
5. **Choi M, Scholl UI, Yue P, et al.** K+ channel mutations in adrenal aldosterone-producing adenomas and hereditary hypertension. *Science*. 2011;331:768–772.
6. **Scholl UI, Nelson-Williams C, Yue P, et al.** Hypertension with or without adrenal hyperplasia due to different inherited mutations in the potassium channel KCNJ5. *Proc Natl Acad Sci USA*. 2012;109:2533–2538.
7. **Mulatero P, Tauber P, Zennaro MC, et al.** KCNJ5 mutations in European families with nonglucocorticoid remediable familial hyperaldosteronism. *Hypertension*. 2012;59:235–240.
8. **Scholl UI, Goh G, Stolting G, et al.** Somatic and germline CACNA1D calcium channel mutations in aldosterone-producing adenomas and primary aldosteronism. *Nat Genet*. 2013;45:1050–1054.
9. **Scholl UI, Stolting G, Nelson-Williams C, et al.** Recurrent gain of function mutation in calcium channel CACNA1H causes early-onset hypertension with primary aldosteronism. *eLife*. 2015;4.
10. **Ye P, Mariniello B, Mantero F, Shibata H, Rainey WE.** G-protein-coupled receptors in aldosterone-producing adenomas: a potential cause of hyperaldosteronism. *J Endocrinol*. 2007;195:39–48.
11. **Gazdar AF, Oie HK, Shackleton CH, et al.** Establishment and characterization of a human adrenocortical carcinoma cell line that expresses multiple pathways of steroid biosynthesis. *Cancer Res*. 1990;50:5488–5496.
12. **Rainey WE, Bird IM, Mason JI.** The NCI-H295 cell line: a pluripotent model for human adrenocortical studies. *Mol Cell Endocrinol*. 1994;100:45–50.
13. **Lesouhaitier O, Chiappe A, Rossier MF.** Aldosterone increases T-type calcium currents in human adrenocarcinoma (H295R) cells by inducing channel expression. *Endocrinology*. 2001;142:4320–4330.
14. **Somekawa S, Imagawa K, Naya N, et al.** Regulation of aldosterone and cortisol production by the transcriptional repressor neuron restrictive silencer factor. *Endocrinology*. 2009;150:3110–3117.
15. **Parmar J, Key RE, Rainey WE.** Development of an adrenocorticotropin-responsive human adrenocortical carcinoma cell line. *J Clin Endocrinol Metab*. 2008;93:4542–4546.
16. **Wang T, Rainey WE.** Human adrenocortical carcinoma cell lines. *Mol Cell Endocrinol*. 2012;351:58–65.
17. **Wang T, Rowland JG, Parmar J, Nesterova M, Seki T, Rainey WE.**

Comparison of aldosterone production among human adrenocortical cell lines. *Horm Metab Res*. 2012;44:245–250.
18. **Oki K, Plonczynski MW, Luis Lam M, Gomez-Sanchez EP, Gomez-Sanchez CE.** Potassium channel mutant KCNJ5 T158A expression in HAC-15 cells increases aldosterone synthesis. *Endocrinology*. 2012;153:1774–1782.
19. **Clyne CD, Nguyen A, Rainey WE.** The effects of KN62, a Ca2+/calmodulin-dependent protein kinase II inhibitor, on adrenocortical cell aldosterone production. *Endocr Res*. 1995;21:259–265.
20. **Martin RL, Lee JH, Cribbs LL, Perez-Reyes E, Hanck DA.** Mibefradil block of cloned T-type calcium channels. *J Pharmacol Exp Ther*. 2000;295:302–308.
21. **Rossier MF, Ertel EA, Vallotton MB, Capponi AM.** Inhibitory action of mibefradil on calcium signaling and aldosterone synthesis in bovine adrenal glomerulosa cells. *J Pharmacol Exp Ther*. 1998;287:824–831.
22. **Vitko I, Bidaud I, Arias JM, Mezghrani A, Lory P, Perez-Reyes E.** The I-II loop controls plasma membrane expression and gating of Ca(v)3.2 T-type Ca2+ channels: a paradigm for childhood absence epilepsy mutations. *J Neurosci*. 2007;27:322–330.
23. **Mor M, Beharier O, Levy S, et al.** ZnT-1 enhances the activity and surface expression of T-type calcium channels through activation of Ras-ERK signaling. *Am J Physiol Cell Physiol*. 2012;303:C192–C203.
24. **Mizuguchi H, Xu Z, Ishii-Watabe A, Uchida E, Hayakawa T.** IRES-dependent second gene expression is significantly lower than cap-dependent first gene expression in a bicistronic vector. *Mol Ther*. 2000;1:376–382.
25. **Spat A, Hunyady L.** Control of aldosterone secretion: a model for convergence in cellular signaling pathways. *Physiol Rev*. 2004;84:489–539.
26. **Lin TC, Chien SC, Hsu PC, Li LA.** Mechanistic study of polychlorinated biphenyl 126-induced CYP11B1 and CYP11B2 up-regulation. *Endocrinology*. 2006;147:1536–1544.
27. **Akizuki O, Inayoshi A, Kitayama T, et al.** Blockade of T-type voltage-dependent Ca2+ channels by benidipine, a dihydropyridine calcium channel blocker, inhibits aldosterone production in human adrenocortical cell line NCI-H295R. *Eur J Pharmacol*. 2008;584:424–434.
28. **Clyne CD, Zhang Y, Slutsker L, Mathis JM, White PC, Rainey WE.** Angiotensin II and potassium regulate human CYP11B2 transcription through common cis-elements. *Mol Endocrinol*. 1997;11:638–649.
29. **Perez-Reyes E.** Molecular physiology of low-voltage-activated t-type calcium channels. *Physiol Rev*. 2003;83:117–161.
30. **Hu C, Rusin CG, Tan Z, Guagliardo NA, Barrett PQ.** Zona glomerulosa cells of the mouse adrenal cortex are intrinsic electrical oscillators. *J Clin Invest*. 2012;122:2046–2053.
31. **Imagawa K, Okayama S, Takaoka M, et al.** Inhibitory effect of efonidipine on aldosterone synthesis and secretion in human adrenocarcinoma (H295R) cells. *J Cardiovasc Pharmacol*. 2006;47:133–138.
32. **Po AL, Zhang WY.** What lessons can be learnt from withdrawal of mibefradil from the market? *Lancet*. 1998;351:1829–1830.
33. **Welker HA.** Single- and multiple-dose mibefradil pharmacokinetics in normal and hypertensive subjects. *J Pharm Pharmacol*. 1998;50:983–987.
34. **Ragueneau I, Sao AB, Demolis JL, Darne B, Funck-Brentano C, Jaillon P.** Comparison of sympathetic modulation induced by single oral doses of mibefradil, amlodipine, and nifedipine in healthy volunteers. *Clin Pharmacol Ther*. 2001;69:122–129.
35. **Schmitt R, Kleinbloesem CH, Belz GG, et al.** Hemodynamic and humoral effects of the novel calcium antagonist Ro 40–5967 in patients with hypertension. *Clin Pharmacol Ther*. 1992;52:314–323.
36. **Azizan EA, Poulsen H, Tuluc P, et al.** Somatic mutations in ATP1A1 and CACNA1D underlie a common subtype of adrenal hypertension. *Nat Genet*. 2013;45:1055–1060.
37. **Tanaka T, Tsutamoto T, Sakai H, Fujii M, Yamamoto T, Horie M.** Comparison of the effects of efonidipine and amlodipine on aldosterone in patients with hypertension. *Hypertens Res*. 2007;30:691–697.
38. **Tsutamoto T, Tanaka T, Nishiyama K, et al.** Long-term effect of efonidipine therapy on plasma aldosterone and left ventricular mass index in patients with essential hypertension. *Hypertens Res*. 2009;32:670–674.